RSC Advances

ROYAL SOCIETY OF CHEMISTRY

www.rsc.org/advances

Cite this: DOI: 10.1039/c0xx00000x

www.rsc.org/xxxxxx

ARTICLE TYPE

Single-step synthesis of DME from syngas on CuZnAl/zeolite bifunctional catalysts: The influence of zeolite type

Qinglong Xie,[a] Paul Chen,[a] Pu Peng,[a] Shiyu Liu,[a] Peng Peng,[a] Bo Zhang,[a] Yanling Cheng,[a,b] Yiqin Wan,[a,c] Yuhuan Liu[a,c] and Roger Ruan*[a,c]

Received (in XXX, XXX) Xth XXXXXXXXX 20XX, Accepted Xth XXXXXXXXX 20XX
DOI: 10.1039/b000000x

In this study, single-step synthesis of DME from syngas on bifunctional catalysts containing Cu-ZnO-Al_2O_3 and seven different zeolites was investigated. Various characterization techniques were used to determine the structure, reducibility, and surface acidity of the catalysts. The experimental results showed that the zeolite type had great influence on the activity, selectivity and stability of the bifunctional catalyst during the syngas-to-DME process. Zeolite properties including density of weak and strong acid sites, pore structure, and Si/Al distribution were found to affect the CO conversion and DME selectivity of the bifunctional catalyst. In addition, the deactivation of the bifunctional catalyst could be attributed to the sintering of metallic Cu and a loss of the zeolite dehydration activity.

Introduction

Dimethyl ether (DME) as an alternative to diesel fuel attracts increasing interest due to its high cetane number (55–60), low auto-ignition temperature, and reduced emissions of pollutants such as CO, NO_x, SO_x, and particulate matter on its combustion.[1–3] DME is an important feedstock in the production of chemicals such as dimethyl sulfate and methyl acetate, as well as ethers and oxygenates. Moreover, DME can be utilized as a residential fuel replacing liquefied petroleum gas (LPG) or propane since they have similar physical properties, or as a feedstock for hydrogen production due to its high H/C ratio and energy density.[2] In addition, the boiling point of DME is very low (–24 ºC), thus it can be used as a low-temperature solvent and extraction agent, which is applicable to certain laboratory procedures.

Traditionally, DME is produced using fossil fuels as the raw materials such as natural gas, coal, and oil. These sources need to be firstly converted to syngas using various gasifying agents like air, oxygen, and steam. After purification and conditioning, the syngas is then converted to methanol followed by its dehydration to DME on certain catalysts. Recently, the utilization of biomass as the feedstock for syngas production has attracted considerable interest,[4] since biomass is a CO_2 neutral and extensively distributed resource in the world.[5] However, the composition of biomass-derived syngas varies with different raw materials, reactor types, temperatures, and other process parameters.[6–8]

DME is conventionally produced using a two-step process comprising synthesis of methanol from syngas on a Cu-ZnO-based catalyst and methanol dehydration to DME on a solid acid catalyst.[9] However, the step of syngas to methanol is limited by the thermodynamic equilibrium, making the overall conversion rate very low.[10] A new single-step synthesis of DME directly from syngas has gained much attention due to its thermodynamic and economic advantages.[10–12] The main reactions involved in the single-step process are represented by equations (1)–(4), assuming that syngas simply consists of H_2 and CO.

Methanol synthesis reaction:

$$2H_2 + CO \leftrightarrow CH_3OH \quad (1)$$

$$3H_2 + CO_2 \leftrightarrow CH_3OH + H_2O \quad (2)$$

Methanol dehydration reaction:

$$2CH_3OH \leftrightarrow CH_3OCH_3 + H_2O \quad (3)$$

Water-gas shift (WGS) reaction:

$$CO + H_2O \leftrightarrow H_2 + CO_2 \quad (4)$$

The equilibrium limitation existing in syngas to methanol process could be overcome through reaction (3) which consumes methanol and shifts the chemical equilibrium of reactions (1) and (2) to the right-hand side. Therefore, more syngas could be utilized and the overall conversion rate is improved. Moreover, the water formed in reactions (2) and (3) reacts with CO through the WGS reaction (equation (4)) and produce H_2 and CO_2, which are reactants of the reaction (2) for methanol synthesis. It can be seen from the above reactions that a bifunctional catalyst is required for the single-step of synthesis of DME from syngas. The catalyst should be able to simultaneously catalyze both the methanol synthesis and the methanol dehydration reactions. The bifunctional catalyst typically consists of a Cu-ZnO-based component for the conversion of syngas to methanol and a solid acid component for the methanol dehydration to DME.

Extensive studies have been conducted on methanol synthesis reaction. Cu-ZnO-based catalyst is reported to be the best for methanol production from syngas. However, the methanol dehydration process has received comparatively less attention. From previous studies, γ-Al_2O_3[13–15] and zeolites[16–19] are the most

common used catalysts as the solid acid component for the DME synthesis. It is widely accepted that γ-Al_2O_3 undergoes a rapid and irreversible deactivation,[20] while zeolites exhibit much higher activity and stability during the methanol dehydration reaction.[21, 22] In addition, the acidic properties and reaction activity of the solid acid component could be affected when it is mixed with the Cu-ZnO-based catalyst. Therefore, it is important and essential to examine the influence of different zeolites on the activity of the bifunctional catalysts and thus the efficiency of the single-step synthesis of DME from syngas.

In this study, seven different zeolites mixed with Cu-ZnO-Al_2O_3 (CZA) were used as the bifunctional catalysts for the single-step synthesis of DME from syngas. Various catalyst characterization techniques including X-ray diffraction (XRD), temperature-programmed reduction (TPR), and temperature-programmed desorption of ammonia (NH_3-TPD) were employed to examine the properties of the bifunctional catalysts. The influence of zeolite type on the overall activity, selectivity, and stability of the bifunctional catalyst during the syngas-to-DME process was investigated.

Materials and methods

Catalyst preparation

The CuO-ZnO-Al_2O_3 functioning as the precursor for the methanol synthesis catalyst was prepared using coprecipitation method described by Baltes et al.[23] A solution of metal nitrates [$Cu(NO_3)_2$ (0.6 mol/L), $Zn(NO_3)_2$ (0.3 mol/L), and $Al(NO_3)_3$ (0.1 mol/L)] and a solution of Na_2CO_3 (1 mol/L) were simultaneously pumped at a constant flow rate of 5 ml/min into a stirred and heated glass reactor with a starting volume of 200 ml of deionized water. During the precipitation process, the reactor was kept at a constant temperature of 70±1 ºC and a constant pH of 7.0±0.1. After the addition of the metal nitrates solution, the suspension was aged for 1h at the same temperature. The pH was also kept constant at 7.0 during the aging process through the controlled addition of the metal nitrates or sodium carbonate solutions. Subsequently, the precipitate was filtered and exhaustively washed with deionized water, and then dried at 105 ºC for 12 h. After grinding to the size of smaller than 1 mm, the dried hydroxyl carbonate precursor was calcined at 300 ºC under air for 3 h, yielding the oxide catalyst precursor.

Four types of commercial zeolites namely, H-ZSM-5, H-Y, H-Beta, and H-Ferrierite purchased from Zeolyst International (Conshohocken, PA) were used as the solid acid component in the preparation of bifunctional catalysts. ZSM-5, Beta and Ferrierite zeolites were provided in their ammonium form and they were calcined at 550 ºC in air for 5 h to their active hydrogen form prior to use.

The bifunctional catalysts were prepared by physically mixing the Cu-ZnO-Al_2O_3 and zeolite components, with CZA/zeolite mass ratio kept at 2:1.

Catalyst characterization

The Brunauer-Emmett-Teller (BET) surface areas of the zeolites were estimated from nitrogen adsorption isotherm data obtained on a Micromeritics ASAP 2000 physisorption analyzer.

The powder X-ray diffraction (XRD) patterns, obtained on a Bruker-AXS (Siemens) D5005 X-ray diffractometer instrument with a Cu–K_α radiation at 45 kV and 40 mA, were used to identify the major crystalline phases present in the CZA-Zeolite bifunctional catalysts and their crystallinity. Data collected from the instrument were analyzed using software MDI Jade 8.0.

The reduction behavior of the CZA oxide precursor was investigated through the temperature-programmed reduction (TPR) experiments carried out with a ChemBET Pulsar TPR/TPD automated chemisorption flow analyzer (Quantachrome Instruments). About 30 mg of sample was initially flushed with He at 350 ºC for 2 h to remove the adsorbed water and other contaminants followed by being cooled to 50 ºC. The gas was then switched to the reductive mixture of 5 vol% H_2 in Ar at a flow rate of 30 ml/min and the temperature was linearly increased up to 600 ºC at a heating rate of 10 ºC/min and kept at 600 ºC for 30 min. The effluent gas flowed through a molecular sieve trap with the generated water removed, and was then analyzed by GC equipped with a thermal conductivity detector (TCD).

The acid properties of the bifunctional catalysts were determined by the temperature-programmed desorption of ammonia (NH_3-TPD) profiles obtained in a ChemBET Pulsar TPR/TPD automated chemisorption flow analyzer (Quantachrome Instruments). Prior to ammonia adsorption, ca. 100 mg of sample was degassed under a He flow at 250 ºC for 2 h. After being cooled to 100 ºC, the sample was saturated with anhydrous NH_3 for about 20 min. The sample was then purged with He to remove excess NH_3 from the sample surface. Finally, the TPD measurement was performed by heating the sample from 100 to 650 ºC at a heating rate of 10 ºC/min under a He flow.

Catalytic synthesis experiments

The single-step synthesis of DME from syngas was conducted in a 316 stainless-steel fixed-bed reactor with a diameter of 12.7 mm charged with 6.0 g of bifunctional catalyst. Prior to reaction, the CuO in the CZA oxide precursor needs to be reduced to its active metallic Cu state by catalyst exposure to a diluted H_2 flow (5 vol% H_2 in N_2) at 245 ºC for 10 h. The gaseous feed stream with H_2/CO volumetric ratio at 2:1 was introduced into the reactor, using two mass flow controllers to precisely control their flow rates separately. The DME synthesis reaction was carried out at temperature of 260 ºC, pressure of 50 bar, and space velocity of 1500 $mL_{syngas}/(g_{cat}$ h). The pressure of the system was controlled using a back pressure regulator set at the end of the reactor. The effluent products were analyzed by a Varian CP-4900 micro gas chromatograph equipped with a 5Å molecular sieve column for the analysis of H_2 and CO, and simultaneously with a PoraPlot Q column for the analysis of CO_2, methanol and DME. The columns were connected to a thermal conductivity detector (TCD) and helium was used as the carrier gas. The CO conversion and products selectivity were calculated based on the total carbon mass balance. The data shown in this study are the averaged values in the range of 15–25 h on stream, with the results representing stable CO conversion and products selectivity.

Results and discussion

Characterization of catalysts

Cite this: DOI: 10.1039/c0xx00000x

www.rsc.org/xxxxxx

ARTICLE TYPE

Table 1 Physicochemical properties of the zeolites

Product name	Type	Framework type	Si/Al ratio	Pore size (Å)	BET surface area (m^2/g)
CBV28014	H-ZSM-5	MFI	280	5.6×5.3, 5.5×5.1	400
CBV8014	H-ZSM-5	MFI	80	5.6×5.3, 5.5×5.1	425
CBV3024E	H-ZSM-5	MFI	30	5.6×5.3, 5.5×5.1	405
CBV400	H-Y	FAU	5.1	7.4×7.4	730
CBV780	H-Y	FAU	80	7.4×7.4	780
CP811C-300	H-Beta	BEA	300	7.6×6.4, 5.6×5.6	620
CP914C	H-Ferrierite	FER	20	4.2×5.4, 3.5×4.8	400

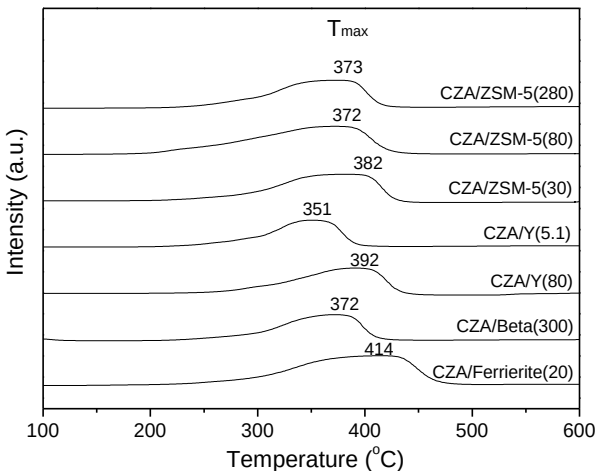

Fig. 1 TPR profiles for the bifunctional catalysts.

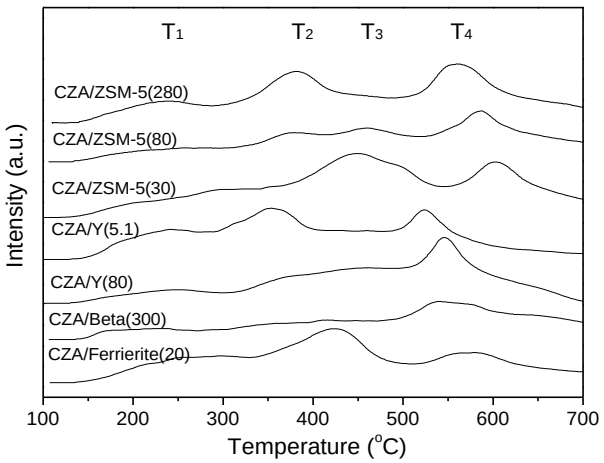

Fig. 2 NH_3-TPD profiles for the bifunctional catalysts.

The physicochemical properties of the zeolites used in this study are summarized in Table 1. It is noticed that the zeolites of H-Y type have larger surface area and pore size than those of other zeolite types. It is reported that the structure plays an important role in maintaining the catalyst stability.[24] The bifunctional catalysts were denoted as CZA/Z(Si:Al), where Z and Si:Al are the type and Si/Al ratio of the zeolites, respectively. For instance, the bifunctional catalyst denoted as CZA/ZSM-5(280) refers to the catalyst prepared by mixing the Cu-ZnO-Al_2O_3 and CBV28014 zeolite.

The H_2-TPR profiles for the seven bifunctional catalysts are shown in Fig. 1. A single reduction feature peak can be observed for the TPR profiles of all the bifunctional catalysts. The temperature of peak maximum (T_{max}) for the bifunctional catalysts CZA/ZSM-5(280), CZA/ZSM-5(80), CZA/ZSM-5(30), CZA/Y(5.1), CZA/Y(80), CZA/Beta(300), and CZA/Ferrierite(20) appears at 373 ºC, 372 ºC, 382 ºC, 351 ºC, 392 ºC, 372 ºC, and 414 ºC, respectively. Therefore, the nature of zeolite has great influence on the overall reducibility of the bifunctional catalysts. However, it is reported that the reduction of copper species occurs at about 205 ºC,[10] and thus, the H_2-reduction treatment at 245 ºC performed in situ prior to reaction is adequate to convert Cu^{2+} to the active metallic Cu.

The NH_3-TPD profiles for the seven bifunctional catalysts are displayed in Fig. 2. Three or four desorption peaks, which appear in the temperature regions of 230–270 ºC (T_1), 350–430 ºC (T_2), 450–490 ºC (T_3), and 520–610 ºC (T_4), respectively, were observed for the catalysts. The desorption peak at lower temperature (T_1) is attributed to the acidity in the zeolite matrix alone and hence it represents weak acid sites, while the peaks at higher temperatures (T_2, T_3 and T_4) are contributed by the acidity on the surface of the zeolite and thus they are assigned to relatively strong acid sites.[25] The density of acid sites for each peak was calculated by comparing the area under the peak with those of the calibration peaks obtained by injecting known amount of ammonia. As shown in Table 2, the amounts of weak, strong and total acid sites on CZA/ZSM-5(30), CZA/Y(5.1), and CZA/Ferrierite(20) are larger than the other bifunctional catalysts. The weak acid sites play an important role for the methanol dehydration activity of the catalyst, however, high density of strong acid sites could facilitate the water-gas shift (WGS) reaction for CO_2 production.[25]

Catalytic synthesis experiments

The results of single-step synthesis of DME from syngas using different zeolites as the solid acid component for the bifunctional catalysts are summarized in Table 3. Higher CO conversion and DME yield could be obtained when ZSM-5(30), or Y(5.1), or Ferrierite(20) was used than when the other zeolites were used. Careful examination of product selectivity reveals a low CH_3OH

Table 2 Surface acidity of the bifunctional catalysts as determined by NH_3-TPD

Catalyst	Density of acid sites (μmol NH_3/g)					Density of acid sites (μmol NH_3/g)		
	T_1	T_2	T_3	T_4	Total	Weak	Strong	Total
CZA/ZSM-5(280)	465.8	266.4	–	242.6	974.8	465.8	509.0	974.8
CZA/ZSM-5(80)	345.5	128.2	284.8	225.1	983.6	345.5	638.1	983.6
CZA/ZSM-5(30)	955.6	–	961.4	518.9	2435.9	955.6	1480.3	2435.9
CZA/Y(5.1)	722.2	547.4	–	434.7	1704.3	722.2	982.1	1704.3
CZA/Y(80)	432.8	205.6	221.0	338.7	1198.1	432.8	765.3	1198.1
CZA/Beta(300)	337.3	383.0	–	364.4	1084.7	337.3	747.4	1084.7
CZA/Ferrierite(20)	720.0	679.8	–	344.3	1744.1	720.0	1024.1	1744.1

Table 3 The influence of different zeolites on single-step synthesis of DME from syngas

Catalyst	CO conversion	Selectivity (%)			DME yield
	(%)	DME	CH_3OH	CO_2	($g \cdot kg_{cat}^{-1} \cdot h^{-1}$)
CZA/ZSM-5(280)	44.6	70.4	24.5	5.2	161.0
CZA/ZSM-5(80)	65.5	62.9	24.9	12.3	211.2
CZA/ZSM-5(30)	87.8	65.9	3.4	30.7	297.0
CZA/Y(5.1)	91.9	63.9	3.0	33.1	301.7
CZA/Y(80)	50.6	23.3	64.5	12.2	60.6
CZA/Beta(300)	30.0	25.9	64.1	9.9	40.0
CZA/Ferrierite(20)	93.0	61.4	2.8	35.8	293.4

Table 4 Pore structures of different types of zeolites

Zeoilte type	Pore structure
H-ZSM-5	3-Dimensional pore system; straight 10-member-ring channels connected by sinusoidal channels
H-Y	3-Dimensional pore structure; circular 12-member-ring windows connected by spherical cavities
H-Beta	3-Dimensional pore system; 12-ring channel in c direction plus two 12-ring channels in a direction perpendicular to c direction
H-Ferrierite	Orthorhombic pore structure; 10-member-ring channels perpendicularly intersected with 8-member-ring channels

content and high DME/CH_3OH selectivity ratio in the product for these three zeolites. The distinct activity and selectivity behavior of the seven bifunctional catalysts can be determined by multiple parameters, such as reducibility, surface acidity, elemental composition, and pore structure of the catalyst.

The reducibility of the Cu species is reported to have great influence on the CO hydrogenation activity.[25] However, no obvious correlation was found between CO conversion and the peak temperature (T_{max}) of the TPR profiles for the bifunctional catalysts. It means that, in this study, the syngas-to-DME process is not controlled by the reduction behavior of the catalyst which probably due to the complete conversion of Cu^{2+} to Cu^0 under the H_2-reduction pretreatment.

The methanol dehydration activity of the bifunctional catalyst is mainly determined by the surface acidity especially the density of weak acid sites on the catalyst. Larger amounts of weak acid sites mean higher activity of the catalyst for methanol dehydration to DME, resulting in higher selectivity to DME and lower selectivity to methanol. This is the most important reason for the high DME selectivity on CZA/ZSM-5(30), CZA/Y(5.1), and CZA/Ferrierite(20). However, the high DME selectivity on CZA/ZSM-5(280) and CZA/ZSM-5(80) is probably due to other factors which will be discussed later. When the overall syngas-to-DME reaction is controlled by the methanol dehydration step, a higher methanol dehydration activity of the bifunctional catalyst,

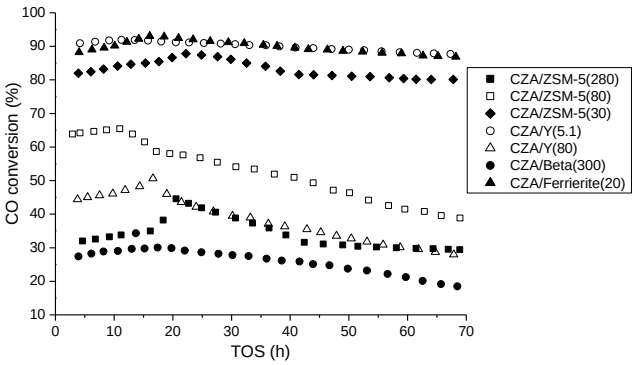

Fig. 3 CO conversion as a function of time on stream (TOS) in syngas-to-DME experiments using different bifunctional catalysts.

which would facilitate the CO/CO_2 hydrogenation by shifting the chemical equilibrium of reactions (1) and (2) to the right-hand side, leads to a higher CO conversion.[10,13] In addition, a high density of strong acid sites on the catalyst could favor the CO_2 formation from CO through the WGS reaction, which further increases the CO conversion. Therefore, the high surface acidity is responsible for the high CO conversion and CO_2 selectivity observed for CZA/ZSM-5(30), CZA/Y(5.1), and CZA/Ferrierite(20) during the syngas-to-DME process.

Pore structure is another important factor that affects catalyst activity and selectivity. The structures of different types of zeolites are given in Table 4.[26] It is likely that the peculiar channel structure of H-Ferrierite facilitates the diffusion and transfer of reaction products. Therefore, the chemical equilibrium of reactions (1)–(3) can be further shifted to the right-hand side, allowing high CO conversion and DME selectivity over CZA/Ferrierite(20) to be attained. In contrary, the peculiar channel structure of H-Beta probably blocks and restricts the transportation of CH_3OH and DME, making the syngas to methanol process easily reach the thermodynamic equilibrium which would result in low CO conversion and DME selectivity.

Si/Al distribution is considered as the most important crystalchemical feature of the zeolite framework, affecting particularly its catalytic properties.[27] Comparing the three H-ZSM-5 zeolites with different Si/Al ratio, it can be found that the lowest CO conversion but highest DME selectivity was obtained when ZSM-5(280) with the highest Si/Al ratio was used. Higher Si/Al ratio would be expected to lead to higher reaction rate due to more catalytically active sites and lower activation barrier.[28] Thus the reaction activity for methanol dehydration is high over the zeolite with high Si/Al ratio, resulting in high DME selectivity. The low CO conversion for the zeolite with high

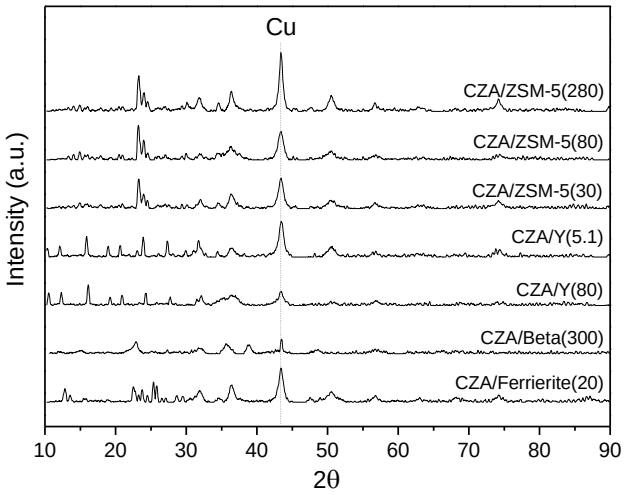

Fig. 4 XRD patterns of bifunctional catalysts after reaction.

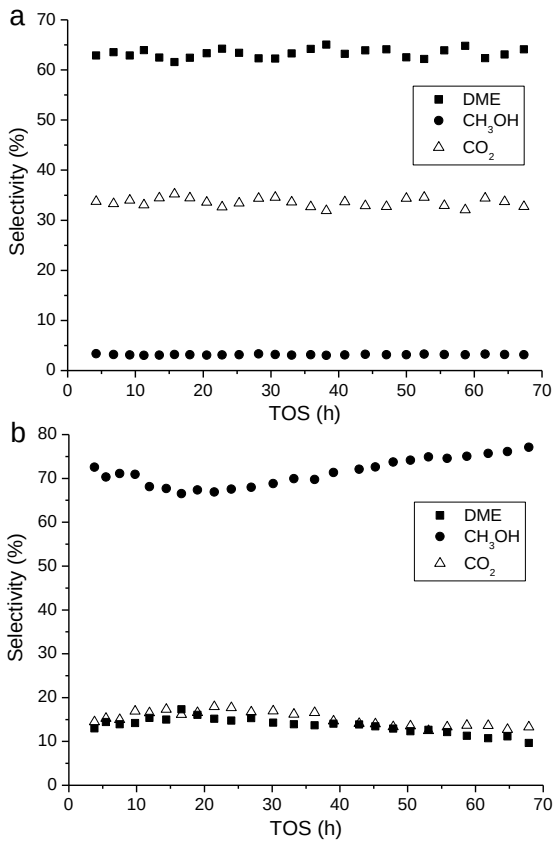

Fig. 5 Selectivity to the main reaction products as a function of TOS in syngas-to-DME experiments on bifunctional catalysts (a) CZA/Y(5.1) and (b) CZA/Y(80).

Si/Al ratio is probably because of the diffusion barrier within the pore channels of zeolite. In addition, it is reported that the catalytic activity does not depend on the Si/Al ratio for H-Y zeolite.[29] Therefore, the CO conversion and DME selectivity on such type of zeolite are mainly determined by the copper activity and surface acidity.

The stability of the bifunctional catalyst is also influenced by the zeolite type. The CO conversion as a function of time on stream (TOS) in syngas-to-DME experiments over the seven bifunctional catalysts is presented in Fig. 3. The results obtained for catalyst stability are basically the same as those for CO conversion on the seven catalysts. Higher stability is observed for CZA/Y(5.1), CZA/Ferrierite(20), and CZA/ZSM-5(30) with lower deactivation rate compared with that for the other bifunctional catalysts. The most obvious deactivation is observed for CZA/Y(80).

The bifunctional catalysts after the 70 h run were characterized and compared using X-ray diffraction (XRD) technique to examine the structure change of the catalysts. As shown in Fig. 4, the characteristic peaks of corresponding zeolite can be observed for each type of bifunctional catalyst, meaning that the zeolite structures were retained during the syngas-to-DME process. However, distinct diffraction peaks occur at the diffraction angles of 43.5° which corresponds to metallic Cu. The intensity of the diffraction peak varies for different bifunctional catalysts after reaction. The crystalline sizes of metallic Cu for the seven catalysts, as estimated by the Scherrer equation, were as follows: CZA/ZSM-5(280) (15.8 nm), CZA/ZSM-5(80) (13.4 nm), CZA/ZSM-5(30) (12.3 nm), CZA/Y(5.1) (12.6 nm), CZA/Y(80) (12.7 nm), CZA/Beta(300) (14.5 nm), and CZA/Ferrierite(20) (12.6 nm). Smaller particle sizes were found for CZA/ZSM-5(30), CZA/Y(5.1), and CZA/Ferrierite(20) than the other bifunctional catalysts, indicating a low deactivation rate of metallic Cu. It could explain the high stability of CO conversion on these three catalysts during the syngas-to-DME experiments. However, the small crystalline size of metallic Cu does not mean high stability of CO conversion for the catalyst CZA/Y(80). The deactivation of this catalyst is perhaps attributed to other causes.

The selectivity to the main reaction products as a function of TOS in syngas-to-DME experiments on bifunctional catalysts CZA/Y(5.1) and CZA/Y(80) is displayed in Fig. 5. As shown in Fig 5a, the selectivity values remained almost constant during the 70 h run for CZA/Y(5.1) although the CO conversion slightly decreased with TOS (Fig. 3). It suggests that for CZA/Y(5.1) the main cause for the decease of CO conversion with TOS is the deactivation of the Cu-based methanol synthesis component.[30,31] However, a different selectivity behavior with TOS can be observed for CZA/Y(80), as depicted in Fig. 5b. The selectivity to DME gradually decreased with TOS but that to CH_3OH increased. It can be inferred from the decrease in the DME/CH_3OH selectivity ratio that for CZA/Y(80), in addition to the deactivation of the Cu-based catalyst, the decrease in CO conversion with TOS is largely due to a loss of the zeolite dehydration activity. Therefore, the influence of zeolite type on the stability of the bifunctional catalyst is rendered mainly through the stability of the surface acidity. It can be concluded that the zeolite acidity has a great impact on the activity, selectivity, and stability of the bifunctional catalyst during the single-step synthesis of DME from syngas.

Conclusions

In this study, the influence of the type of zeolite in the CuZnAl/zeolite bifunctional catalysts on the single-step synthesis of DME from syngas was investigated. Seven different zeolites were used to prepare the bifunctional catalysts, which were characterized using XRD, H_2-TPR, and NH_3-TPD techniques. The activity, selectivity and stability behavior of the bifunctional

catalyst during the syngas-to-DME process was found to be affected by the zeolite properties, including surface acidity, pore structure, and Si/Al ratio of zeolite.

Acknowledgements

The authors would like to express their great appreciation to Minnesota Environment and Natural Resources Trust Fund, North Central Regional Sun Grant Center at South Dakota State University through a grant provided by the US Department of Agriculture (2013-38502-21424) and a grant provided by the US Department of Transportation, Office of the Secretary (DTOS59-07-G-00054), and University of Minnesota Center for Biorefining, as well as China Scholarship Council (CSC), High Technology Research and Development Program of China (2012AA021704, 2014AA022002), Beijing Municipal Science and Technology Commission (z141109004414002), International Science and Technology Cooperation Program of China (2014DFA61040), National High-tech R&D Program of China (2012AA021205, 2012AA101809), National Natural Science Foundation of China (21266022) for their financial support for this work. Parts of this work were carried out in the Characterization Facility, University of Minnesota, a member of the NSF-funded Materials Research Facilities Network (www.mrfn.org) via the MRSEC program.

Notes and references

[a] *Center for Biorefining and Department of Bioproducts and Biosystems Engineering, University of Minnesota, 1390 Eckles Ave., St. Paul, MN 55108, USA. Fax: +1 612-624-3005; Tel: +1 612-625-1710; E-mail: ruanx001@umn.edu*

[b] *Biochemical Engineering College, Beijing Union University, No. 18, Fatouxili 3 Area, Chaoyang District, Beijing 100023, China.*

[c] *Ministry of Education Engineering Research Center for Biomass Conversion, Nanchang University, 235 Nanjing Road, Nanchang, Jiangxi 330047, China.*

1 J. Hu, Y. Wang, C. Cao, D. C. Elliott, D. J. Stevens and J. F. White, *Ind. Eng. Chem. Res.*, 2005, **44**, 1722–1727.

2 T. A. Semelsberger, R. L. Borup and H. L. Greene, *J. Power Sources*, 2006, **156**, 497–511.

3 C. Arcoumanis, C. Bae, R. Crookes and E. Kinoshita, *Fuel*, 2008, **87**, 1014–1030.

4 Y. Lv, T. Wang, C. Wu, L. Ma and Y. Zhou, *Biotechnol. Adv.*, 2009, **27**, 551–554.

5 P. Lv, Z. Yuan, C. Wu, L. Ma, Y. Chen and N. Tsubaki, *Energy Convers. Manag.*, 2007, **48**, 1132–1139.

6 M. K. Karmakar and A. B. Datta, *Bioresour. Technol.*, 2011, **102**, 1907–1913.

7 X. Xiao, X. Meng, D. D. Le and T. Takarada, *Bioresour. Technol.*, 2011, **102**, 1975–1981.

8 Q. Xie, S. Kong, Y. Liu and H. Zeng, *Bioresour. Technol.*, 2012, **110**, 603–609.

9 J. J. Spivey, *Chem. Eng. Commun.*, 1991, **110**, 123–142.

10 A. García-Trenco and A. Martínez, *Appl. Catal. A*, 2012, **411–412**, 170–179.

11 F. Hayer, H. Bakhtiary-Davijany, R. Myrstad, A. Holmen, P. Pfeifer and H. J. Venvik, *Chem. Eng. J.*, 2011, **167**, 610–615.

12 Y. Li, T. Wang, X. Yin, C. Wu, L. Ma, H. Li, Y. Lv and L. Sun, *Renew. Energy*, 2011, **35**, 583–587.

13 D. Mao, W. Yang, J. Xia, B. Zhang and G. Lu, *J. Mol. Catal. A*, 2006, **250**, 138–144.

14 G. R. Moradi, S. Nosrati and F. Yaripor, *Catal. Commun.*, 2007, **8**, 598–606.

15 F. Yaripor, F. Baghaei, I. Schmidt and J. Perregaard, *Catal. Commun.*, 2005, **6**, 147–152.

16 J. Ereña, R. Garoña, J. M. Arandes, A. T. Aguayo and J. Bilbao, *Catal. Today*, 2005, **107–108**, 467–473.

17 D. Mao, W. Yang, J. Xia, B. Zhang, Q. Song and Q. Chen, *J. Catal.*, 2005, **230**, 140–149.

18 V. Vishwanathan, K. W. Jun, J. W. Kim and H. S. Roh, *Appl. Catal. A*, 2004, **276**, 251–255.

19 L. Wang, Y. Qi, Y. Wei, D. Fang, S. Meng and Z. Liu, *Catal. Lett.*, 2006, **106**, 61–66.

20 F. Yaripor, F. Baghaei, I. Schmidt and J. Perregaard, *Catal. Commun.*, 2005, **6**, 542–549.

21 T. Takeguchi, K. Yanagisawa, T. Inui and M. Inoue, *Appl. Catal.*, 2000, **192**, 201–209.

22 M. Xu, J. H. Lunsford, D. W. Goodman and A. Bhattacharyya, *Appl. Catal. A*, 1997, **149**, 289–301.

23 C. Baltes, S. Vukojević and F. Schüth, *J. Catal. A*, 2008, **258**, 334–344.

24 D. Jin, B. Zhu, Z. Hou, J. Fei, H. Lou and X. Zheng, *Fuel*, 2007, **86**, 2707–2713.

25 P. S. Sai Prasad, J. W. Bae, S. H. Kang, Y. J. Lee and K. W. Jun, *Fuel Process. Technol.*, 2008, **89**, 1281–1286.

26 A. Aho, N. Kumar, K. Eränen, T. Salmi, M. Hupa and D. Yu. Murzin, *Fuel*, 2008, **87**, 2493–2501.

27 A. Alberti, G. Cruciani, E. Galli, S. Merlino, R. Millini, S. Quartieri, G. Vezzalini and S. Zanardi, *J. Phys. Chem. B*, 2002, **106**, 10277–10284.

28 F. E. Celik, T. J. Kim and A. T. Bell, *J. Catal.*, 2010, **270**, 185–195.

29 B. Xu, S. Bordiga, R. Prins and J. A. van Bokhoven, *Appl. Catal. A*, 2007, **333**, 245–253.

30 Y. Luan, H. Xu, C. Yu, W. Li and S. Hou, *Catal. Lett.*, 2007, **115**, 23–26.

31 F. S. R. Barbosa, V. S. O. Ruiz, J. L. F. Monteiro, R. R. de Avillez, L. E. P. Borges and L. G. Appel, *Catal. Lett.*, 2008, **126**, 173–178.